Food Chemistry: X 19 (2023) 100827

Contents lists available at ScienceDirect

Food Chemistry: X

journal homepage: www.sciencedirect.com/journal/food-chemistry-x

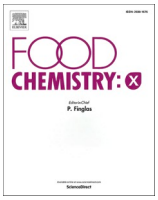

Comparison on structure, properties and functions of pomegranate peel soluble dietary fiber extracted by different methods

Min Xiong [a,1], Mei Feng [a,1], Yanli Chen [a], Shanshan Li [a], Zhengfeng Fang [a], Lina Wang [a], Derong Lin [a], Qing Zhang [a], Yuntao Liu [a], Yuheng Luo [b], Hong Chen [a,*]

[a] College of Food Science, Sichuan Agricultural University, Yaan, Sichuan 625014, China
[b] Institute of Animal Nutrition, Sichuan Agricultural University, Chengdu, Sichuan 611130, China

ARTICLE INFO

Keywords:
Pomegranate peel
Soluble dietary fiber
Extraction methods
Structural properties
Physicochemical properties

ABSTRACT

In this research, the different methods (acid extraction, alkaline extraction and enzymatic extraction) were used to extract soluble dietary fiber (SDF) from pomegranate peel and compared with water extraction. Results revealed that all three extraction methods influenced the structure, physicochemical and functional properties of SDF. Especially, SDF extracted by enzymes (E-SDF) and SDF extracted by alkali (A-SDF) had higher yield (27.30% and 27.17%), molecular weight and thermal stability than SDF extracted by water (W-SDF). Higher oil holding capacity (OHC) was found in SDF extracted by acid (C-SDF) (3.18 g/g), A-SDF (3.18 g/g) and E-SDF (5.36 g/g) compared with W-SDF. In addition, A-SDF showed the smallest particle size, lowest ζ-potential and highest viscosity among the tested samples. E-SDF presented a more porous structure, better glucose adsorption capacity (GAC) and antioxidant activity than C-SDF and A-SDF. To sum up, A-SDF and E-SDF may have great potential to be functional food ingredients in the food industry.

1. Introduction

Dietary fiber is a class of carbohydrate polymer which can not be hydrolyzed by endogenous digestive enzymes in small intestine but can fermented by gut microbiota in large intestine completely or partially (Zheng et al., 2021). As a major functional component or bioactive compound in food, dietary fiber not only has many benefits to human health but also plays an important role in food processing (Du et al., 2021; Wang, Li, Wang, Liu, & Ni, 2021). On the basis of the solubility of dietary fiber in water, it can be divided into soluble dietary fiber (SDF) and insoluble dietary fiber (IDF). Among them, IDF includes cellulose, hemicellulose and lignin, whereas SDF includes gums, mucilage and pectic substances (Cheng, Zhang, Hong, Li, Li, & Gu, 2017). SDF is commonly served as a functional food component applied to the food industry on account of its superior solubility and water/oil holding capacity (Moczkowska, Karp, Niu, & Kurek, 2019). To improve the mouthfeel of food and enhance the storage stability of food, SDF can also be used as an emulsifier, thickener, stabilizer and fat substitute in the food industry (Gu, Fang, Gao, Su, Niu, & Yu, 2020). Furthermore, SDF has strong antioxidant activity and can lower blood glucose, blood pressure and cholesterol levels, thereby helping alleviate some diseases, such as diabetes, cardiovascular disease, hyperlipidemia and colon cancer (Bader Ul Ain, Saeed, Ahmed, Asif Khan, Niaz, & Tufail, 2019). To date, the main sources of SDF are cereals, legumes, nuts, fruits and vegetables (Bader Ul Ain et al., 2019). Obtaining SDF from fruit and vegetable by-products has received increasing attention by researchers in the field (O'Shea, Arendt, & Gallagher, 2012).

As the main by-product of pomegranate eating and processing, pomegranate peel accounts for about 50% of the fruit weight. A growing number of active substances, which are beneficial to health and promote food processing, are prepared from pomegranate peel. Research shows that the dietary fiber in pomegranate peel accounts for about 47% and mainly comprises SDF (Hasnaoui, Wathelet, & Jimenez-Araujo, 2014). SDF extraction from pomegranate peel can improve the utilization of pomegranate by-product and increase economic benefits. However, research on the extraction of SDF from pomegranate peels is limited.

Current methods for extracting SDF mainly include chemical, physical and biological techniques, which can break some insoluble glycosidic bonds to a certain extent and improve the extraction rate of SDF (Jia et al., 2019). The chemical method and enzymatic method are easy

* Corresponding author.
E-mail address: chenhong945@sicau.edu.cn (H. Chen).
[1] Min Xiong, Mei Feng contributed equally to this work as the first authors.

https://doi.org/10.1016/j.fochx.2023.100827
Received 4 April 2023; Received in revised form 1 August 2023; Accepted 4 August 2023
Available online 16 August 2023
2590-1575/© 2023 The Author(s). Published by Elsevier Ltd. This is an open access article under the CC BY-NC-ND license (http://creativecommons.org/licenses/by-nc-nd/4.0/).

to operate and consume low energy; moreover, materials are readily available. In addition, the enzymatic method possesses the advantages of high efficiency and mild conditions. The chemical method is regarded as an important way to improve the solubility of dietary fiber and it can easily enhance SDF yield (Wang et al., 2019). An alkaline solution can break the glycosidic bond in dietary fiber, and acid extraction can effectively hydrolyze hemicellulose, thereby changing the ratio of SDF and IDF (Wang, Xu, Yuan, Fan, & Gao, 2015; Zhang, Qi, Zeng, Huang, & Yang, 2020). By contrast, enzyme extraction can destroy cellulose, hemicellulose and lignin in the cell wall, contributing to the conversion of IDF to SDF (Gan et al., 2020). Different extraction methods can not only change the yield of SDF but also alter the composition and structural properties of SDF and then change its physicochemical and functional properties. Alkali extraction enhances the yield and heat stability of SDF (Huang, Liao, Qi, Jiang, & Yang, 2021; Zhang et al., 2020). SDF extracted by citric acid has high water holding capacity and glucose adsorption ability (Wang et al., 2021). SDF obtained via enzyme extraction possesses low molecular weight, loose structure, good hydration performance and glucose adsorption capacity (Gu et al., 2020).

This study aimed to prepare pomegranate peel SDF by different extraction methods (acid extraction, alkali extraction and enzyme extraction) to obtain high yield of SDF and compare the different extraction on the composition, structure, physicochemical properties and functional characteristics of pomegranate peel SDF. The research offers insight to study on pomegranate peel SDF and provides a theoretical basis for the utilisation of pomegranate peel.

2. Materials and methods

2.1. Materials

Tunisian pomegranates with soft seeds were purchased from Binghuang Technology Development Co., Ltd. (Sichuan Province, China). Papain (800 U/mg), heat-resistant α-amylase (4×10^4 U/g), cellulase (400 U/mg), 1,1-diphenyl-2-picrylhydrazine (DPPH) and p-nitrophenyl-α-D-glucopyranoside (PNPG), which were all chromatographically pure, were procured from Yuanye Biotechnology Co., Ltd. (Shanghai, China). Citric acid, sodium hydroxide, ferric chloride and hydrochloric acid were provided by Chengdu Cologne Chemicals Co., Ltd. (Sichuan Province, China). All the chemical reagents were of analytical grade.

2.2. Preparation of SDF

2.2.1. Pretreatment of pomegranate peels

Pomegranate peels were first separated from the fresh fruits and then exsiccated with an oven at 42 °C for 48 h. After drying, the peels were pulverized with a high-speed crusher (LDP-500A, Yongkang Hongtaiyang Electromechanical Co., Ltd, Zhejiang Province, China), followed by passing through a 60-mesh screen. The prepared sample was hoarded in a dry container at room temperature for further analysis.

2.2.2. Water extraction

Water extraction was accomplished by referring to the protocol for a previous report with minor modification (Gan et al., 2020). The mixture was prepared with 10 g of pomegranate peel powder and distilled water (1:15, w/v) and agitated at ambient temperature for 2 h. Subsequently, the mixture was centrifuged at 4000×g for 20 min to remove water-insoluble materials. The centrifuged supernatant was concentrated prior to precipitating with ethanol and treating with vacuum freeze-drying. The yielded SDF was designated as W-SDF.

2.2.3. Acid extraction

Acid extraction was conducted using a method from a previous study with slight modification (Wang et al., 2021). About 150 mL of citric acid solution (1%, w/v) was intermixed with 10 g of pomegranate peel powder. The successive operations were the same as the descriptions in 2.2.2 to acquire C-SDF.

2.2.4. Alkali extraction

A-SDF was obtained by alkali extraction based on the approach of a previous research (Ding et al., 2020). Pomegranate peel powder with a mass of 10 g was blended into 150 mL of sodium hydroxide solution (1%, w/w). Subsequent processes were in accordance with 2.2.2 to obtain A-SDF.

2.2.5. Enzyme extraction

According to a previous study, SDF extraction was conducted by virtue of hydrolysis of several enzymes (Gan et al., 2020). About 10 g of pomegranate peel powder was suspended in 150 mL of distilled water. The solution was enzymatically hydrolyzed by adding cellulase (80 mg, 400 U/g) for 4 h in the 50 °C water bath, heat-resistant α-amylase (0.1 g, 4×10^4 U/g) for 0.5 h in the 95 °C water bath and papain (5 mg, 800 U/mg) for 0.5 h in the 60 °C water bath. Later, the mixture was incubated boiling water bath for 15 min to inactivate the enzymes. The rest of the steps were the same as those specified in 2.2.2 to attain E-SDF.

2.3. Chemical analysis

In accordance with the AOAC methods, the moisture (method 925.09), ash (method 942.05) and protein (method 960.52) of all samples extracted by diverse means were determined. Pectin was measured by the carbazole colorimetric method (Hui et al., 2009).

2.4. Monosaccharide composition

The monosaccharide composition of SDF was determined by high-performance anion-exchange chromatography (HPAEC, ICS5000, Thermo Fisher Scientific, USA), which comprised a CarboPac PA-20 anion-exchange column (3 × 150 mm; Dionex) and a pulsed amperometric detector (PAD; Dionex ICS 5000 system). The unambiguous operations of monosaccharide analysis were in conformity to the method proposed by a previous study (Gu et al., 2020) with minor modification. The sample was hydrolyzed by 2 mL of trifluoroacetic acid (2 mol/L) at 105 °C for 6 h. About 5 μL of hydrolysis sample solution was injected into the system with a constant column temperature (30 °C) at a flow rate of 0.5 mL/min. The mobile phase was composed of solution A (0.1 mol/L NaOH) and solution B (0.1 mol/L NaOH and 0.2 mol/L NaAc).

2.5. Molecular weight (M_W)

The molecular weight distribution of all samples was analyzed by gel permeation chromatograph (GPC, Agilent 1260, Agilent Technologies, California, USA), and the operation was performed in accordance with a previous report (Jia et al., 2019) with slight modification. About 100 μL of the sample (3 mg/mL) was injected after filtering, and columns were kept at 30 °C for 30 min. The mobile phase was ultrapure water containing 0.1 mol/L $NaNO_3$ and 550 ppm NaN_3. The standard curve was obtained by using a series of dextran T standards (M_W:194 Da–1,046,000 Da). The weight average molecular mass (M_W), number average molar mass (Mn) and polydispersity index (M_W/Mn) were analyzed using Agilent GPC/SEC Software A.02.01 (Agilent Technologies, California, USA).

2.6. Scanning electron microscopy (SEM)

In brief, the samples were dried to constant weight, stuck on the copper strip and equably sprayed with a gold layer. The samples were then examined by scanning electron microscope (SEM SU4800, Hitachi, Tokyo, Japan), and micrographs were captured at different magnifications.

2.7. Fourier transform infrared spectroscopy (FT-IR)

Approximately 1.0 mg of sample and 100 mg of KBr were ground thoroughly and mixed well with each other. The mixture was pressed into sheets, and the slices were assayed using a FT-IR spectrometer (NICOLET IS 10, Thermo Fisher Scientific, USA) in the wavelength range of 4000–500 cm^{-1}.

2.8. Thermal property

The thermogravimetric analysis (TGA) and differential scanning calorimetry (DSC) of SDF were measured by following a previously described procedure (Kurek, Karp, Wyrwisz, & Niu, 2018). TGA and DSC were performed using a thermogravimetric analyzer (TG 209 F3 Nevio, Netzsch, Bavaria, Germany) and differential scanning calorimeter (Q200DSC, TA Instruments, New Castle, USA), respectively. The measurement was operated under an atmosphere of high-pure nitrogen at a flow rate of 20 mL/min. Moreover, the measurement conditions were a heating rate of 20 °C/min over a temperature range of 50–600 °C and a heating rate of 10 °C/min over a temperature range of 20–300 °C for TGA and DSC, respectively.

2.9. Particle size and ζ-potential

The particle size and ζ-potential of SDF were measured with a Dynamic Optical Nanoparticle Particle Size Potentiometer (Zetasizer Nano ZS, Malvern Instruments Co., Ltd., Worcestershire, UK) in accordance with a previous protocol (Huang et al., 2021). 1 g of SDF samples dissolved in deionised water (0.1 g/mL) were analyzed with the software delivered with the system.

2.10. Viscosity

The measurement was carried out according to the method reported by the previous study (Chen et al., 2021). The viscosity of SDF (20%, w/v) was measured by using a rheometer (DHR-1, TA Instruments, New Castle, USA) with a 40 mm parallel plate at 25 °C. Measurements were conducted over a shear rate range of 1–300 s^{-1} and a shear stress range of 1–50 Pa.

2.11. Functional properties

2.11.1. Water solubility (WS)

WS was measured according to a previously described study (Cheng et al., 2017). 1 g of the sample was suspended in 10 mL of deionized water, and the suspension was stirred at ambient temperature for 60 min. The suspension was centrifuged at 6000 × g for 10 min, and the volume of the supernatant was documented. Subsequently, 8 mL of the supernatant was transferred into a tared dish, followed by drying at 105 °C to a constant weight. The solubility of SDF was computed by the equation below.

$$WS\ (\%) = \frac{m_2 - m_1}{m} \times \frac{V}{8} \times 100\% \quad (1)$$

where m is the mass of the SDF sample, m_1 is the mass of the tared dish, m_2 is the mass of the tared dish containing the sample, and V is the volume of the supernatant recorded.

2.11.2. Oil holding capacity (OHC)

OHC was assessed using a method from a previous study (Jia et al., 2019). Peanut oil (10 mL) was blended with the SDF sample (0.5 g) and agitated equably. The suspension was cultured at 37 °C for 1 h prior to centrifuging at 4000 × g for 20 min. The sediment was extracted by spilling the supernatant oil. OHC was computed using the equation below and expressed in gram of oil retained per gram of sample.

$$OHC\ (g/g) = \frac{m_2 - m_1}{m_1} \quad (2)$$

where m_1 is the mass of the SDF sample, and m_2 is the mass of SDF after centrifugation.

2.11.3. Glucose adsorption capacity (GAC)

GAC was evaluated according to the published literature (Xiong et al., 2022). About 1 g of sample was incorporated with 5 mL of glucose solution with diverse concentrations (10, 50, 100 and 200 mmol/L), and the mixture was vibrationally incubated at 37 °C for 6 h. The mixture was centrifuged at 4000×g for 20 min and the supernatant was attained. The glucose content in the supernatant was determined to measure the reducing sugar amount with a glucose assay kit (Nanjing Jiancheng Bioengineering Institute, Nanjing, China). Each sample was prepared in triplicate, and the GAC was calculated by the following equation.

$$GAC = \frac{(C_0 - C_1) \times V}{m} \quad (3)$$

where C_0 is the concentration of glucose prior to adsorption, C_1 is the concentration of glucose in the supernatant after absorption, V is the bulk of glucose solution, and m is the mass of the sample.

2.11.4. Ferric reducing antioxidant power (FRAP)

FRAP was conducted according to a previously reported study (Langley-Evans, 2000). The working solution was confected using 10 mmol/L TPTZ (2,4,6-tripyridyl-s-triazine) solution dissolved in hydrochloric acid (40 mmol/L), ferric chloride solution (20 mmol/L) and sodium acetate buffer (300 mmol/L) at a proportion of 1:1:10. The standard curve was plotted using ferrous sulfate with different concentrations (0.2, 0.4, 0.6, 0.8 and 1.0 mmol/L). Subsequently, 100 μL of sample solution (0.02, 0.04, 0.06, 0.08 and 0.1 mg/mL) was mixed with 900 μL of the working solution and shaken thoroughly and incubated at 37 °C for 10 min. The absorbance of the mixture was determined at 593 nm by a fluorescence microplate reader (Varioskan las, Thermo Fisher Scientific, USA). Results were denoted by the concentration (mmol/L) of ferrous sulfate.

2.11.5. Scavenging of DPPH radical

The capability of extracts to scavenge DPPH radical was assessed using a previously described approach (Wang, Zhang, et al., 2016) with minor modification. SDF was first prepared into solution with five different concentrations (0.03, 0.06, 0.09, 0.12 and 0.15 mg/mL). Subsequently, 1000 μL of DPPH (0.2 mmol/L) and methanol solution were blended with 500 μL of the sample solution in sequence and then shaken rapidly. The mixed solution was incubated in the dark for 30 min, and the absorbance was measured at 517 nm using a fluorescence microplate reader (Varioskan las, Thermo Fisher Scientific, USA). Ascorbic acid was used as the positive control. The activity of scavenging the DPPH radical was calculated as follows.

$$DPPH\ radical\ scavenging\ activity = \frac{A_0 - A_1}{A_0} \times 100\% \quad (4)$$

where A_0 is the absorbance of the blank control, and A_1 is the absorbance of the sample solution.

2.11.6. Scavenging of ABTS radical

The antioxidant capacity of SDF was estimated on the basis of the scavenging activity of ABTS radical (Chen, Chen, Wang, & Kan, 2020). The $ABTS^{\bullet+}$ solution was obtained by mixing ABTS solution (7 mmol/L) with potassium persulfate solution (2.45 mmol/L) at a ratio of 1:1 (v/v). Subsequently, 50 μL of the sample solution (0.01, 0.02, 0.03, 0.04 and 0.05 mg/mL) was mixed with the $ABTS^{\bullet+}$ solution (200 μL). The mixture was incubated in the dark at ambient temperature for 10 min prior to determination by using a fluorescence microplate reader (Varioskan las,

Table 1
DF samples extraction yield and composition (dry basis).

Extraction method	Yield		Chemical composition of SDF			
	IDF(%)	SDF(%)	Moisture (g/100 g)	Ash (g/100 g)	Protein (g/100 g)	Pectin (g/100 g)
water extraction	34.17 ± 0.97^{b}	15.63 ± 2.24^{b}	7.43 ± 0.33^{a}	5.43 ± 0.24b^{c}	1.31 ± 0.10^{b}	10.01 ± 0.05^{b}
acid extraction	36.43 ± 0.29^{a}	10.27 ± 2.26^{c}	7.94 ± 1.17^{b}	3.19 ± 0.35^{d}	0.98 ± 0.25^{b}	2.22 ± 0.11^{c}
alkali extraction	24.23 ± 0.60^{d}	27.17 ± 1.07^{a}	6.99 ± 1.49^{c}	25.19 ± 0.21^{a}	3.26 ± 0.54^{a}	16.08 ± 0.90^{a}
enzyme extraction	31.57 ± 0.76^{c}	27.30 ± 1.66^{a}	6.84 ± 0.35^{d}	6.55 ± 1.39^{b}	1.43 ± 0.27^{b}	9.26 ± 0.16^{b}

Data are expressed as the means ± standard deviation (n = 3). Values in the same column with different letters are significantly different ($p < 0.05$). DF: dietary fiber; IDF: insoluble dietary fiber; SDF: soluble dietary fiber.

Table 2
Monosaccharide composition of SDF samples extracted by different methods.

Monosaccharide (%)	W-SDF	C-SDF	A-SDF	E-SDF
Fucose	0.31	0.14	0.43	0.33
Rhamnose	2.68	1.21	3.03	2.17
Arabinose	8.17	3.71	11.58	6.90
Galactose	5.86	2.91	5.81	4.27
Glucose	62.93	74.25	60.20	65.31
Xylose	0.83	0.61	2.20	1.09
Mannose	0.77	0.68	4.15	1.11
Fructose	0.45	0.33	0.24	0.34
Galacturonic acid	17.07	15.77	11.29	17.90
Glucuronic acid	0.75	0.32	0.70	0.43

The result of the monosaccharide composition is presented as percentage of total monosaccharides; SDF: soluble dietary fiber; W-SDF: soluble dietary fiber extracted by water; C-SDF: soluble dietary fiber extracted by acid; A-SDF: soluble dietary fiber extracted by alkali; E-SDF: soluble dietary fiber extracted by enzymes.

Thermo Fisher Scientific, USA) to gain the absorbance of the mixture at 734 nm. The following formula was used to calculate the scavenging capacity of ABTS radical.

$$ABTS\ radical\ scavenging\ activity = \left(1 - \frac{A_1}{A_0}\right) \times 100 \quad (5)$$

where A_0 is the absorbance of the blank control, and A_1 is the absorbance of the sample solution.

2.12. Statistical analysis

All the experiments were performed in triplicate and data were displayed as mean ± standard deviation (SD). Statistical analysis was performed by SPSS version 22.0 software (IBM Co., USA), and the differences between means were estimated by ANOVA (Duncan's test). $P < 0.05$ was designated as the significant level.

3. Results and discussion

3.1. Extraction yield and composition

The yields of IDF and SDF extracted by different methods are shown in Table 1. Compared with water extraction, alkali and enzyme extraction significantly increased the yield of SDF ($p < 0.05$). This result indicated that the two latter extraction methods could destroy the cell wall of the sample, and the cell contents were released, resulting in the formation of small molecules from polymers (Gu et al., 2020; Wang et al., 2021). By contrast, acid extraction resulted in the lowest content of SDF, suggesting that acid extraction broke down the glycosidic linkages in dietary fiber, leading to the conversion of SDF to low molecular weight monosaccharides and oligosaccharides (Wang et al., 2021). The yields of SDF samples from pomegranate peel were higher than those from tomato peel except for SDF extracted by acid (Niu, Li, Xia, Hou, & Xu, 2018). The above results revealed that alkali and enzyme extraction could effectively enhance the yield of SDF.

Table 3
The molecular weight, particle size, ζ-potential, WS, OHC and GAC of SDF samples extracted by different methods.

	W-SDF	C-SDF	A-SDF	E-SDF
Mn (kDa)	0.837	0.726	1.001	0.732
M_W (kDa)	9.322	8.421	40.228	35.573
M_W / Mn	11.137	11.599	40.188	48.597
Particle size (nm)	409.27 ± 7.05^{b}	397.23 ± 4.91^{b}	204.90 ± 3.01^{c}	586.97 ± 21.58^{a}
ζ-potential (mV)	−28.83 ± 2.29^{b}	−21.33 ± 1.37^{a}	−43.87 ± 0.50^{d}	−33.67 ± 1.23^{c}
WS (%)	93 ± 1.00^{a}	86 ± 8.62^{a}	85 ± 1.16^{a}	90 ± 4.16^{a}
OHC (g/g)	2.89 ± 0.04^{c}	3.18 ± 0.12^{b}	3.18 ± 0.14^{b}	5.36 ± 0.16^{a}
GAC (mmol/g)				
10 mmol/L	0.64 ± 0.02^{a}	0.55 ± 0.02^{b}	0.41 ± 0.01^{c}	0.62 ± 0.03^{a}
50 mmol/L	1.88 ± 0.15^{a}	1.56 ± 0.21^{ab}	1.46 ± 0.04^{b}	1.81 ± 0.11^{a}
100 mmol/L	3.27 ± 0.29^{a}	2.97 ± 0.26^{a}	3.21 ± 0.58^{a}	2.99 ± 0.59^{a}
200 mmol/L	6.08 ± 0.54^{a}	4.15 ± 0.59^{b}	5.62 ± 1.18^{a}	5.36 ± 0.27^{a}

Data are expressed as the means ± standard deviation (n = 3). Values in the same column with different letters are significantly different ($p < 0.05$). Mn: number-average molecular weight; M_W: weight-average molecular weight; WS: water solubility; OHC: oil holding capacity; GAC: glucose adsorption capacity; SDF: soluble dietary fiber; W-SDF: soluble dietary fiber extracted by water; C-SDF: soluble dietary fiber extracted by acid; A-SDF: soluble dietary fiber extracted by alkali; E-SDF: soluble dietary fiber extracted by enzymes.

The composition of SDF is presented in Table 1. A-SDF exhibited the highest content of ash, protein and pectin. The highest amount of ash in A-SDF was observed might due to the ions introduced by chemical reagents (Huang et al., 2021). The increase of pectin amount in A-SDF probably as the result of the dissolution of polymeric networks caused by alkali, thereby contributing to the release of pectin. The result was consistent with the previous study (Wandee, Uttapap, & Mischnick, 2018). By contrast, C-SDF had the lowest content of pectin, resulting from the slight destruction of acid to the bond of pectin with the cell wall (Meng, Wu, Liu, Tang, & Nie, 2021).

3.2. Monosaccharide composition analysis

As shown in Table 2, HPAEC was applied to determine the difference among all SDF samples in monosaccharide composition. All SDF samples comprised ten types of monosaccharides such as fucose, rhamnose, arabinose, galactose, glucose, xylose, mannose, fructose, galacturonic acid and glucuronic acid, which were different from tomato peel SDF in terms of monosaccharide type and content (Niu et al., 2018). Glucose, galacturonic acid, arabinose, galactose and rhamnose were the main monosaccharide constituents of all SDF samples after extraction. Glucose ranked the highest among the five monosaccharides, and most glucose may have come from fiber as the main component in the cell wall of pomegranate peels (Yuliarti, Goh, Matia-Merino, Mawson, & Brennan, 2015). Galacturonic acid, arabinose, galactose and rhamnose were emblematic of pectin, indicating that pectin also existed in SDF (Li,

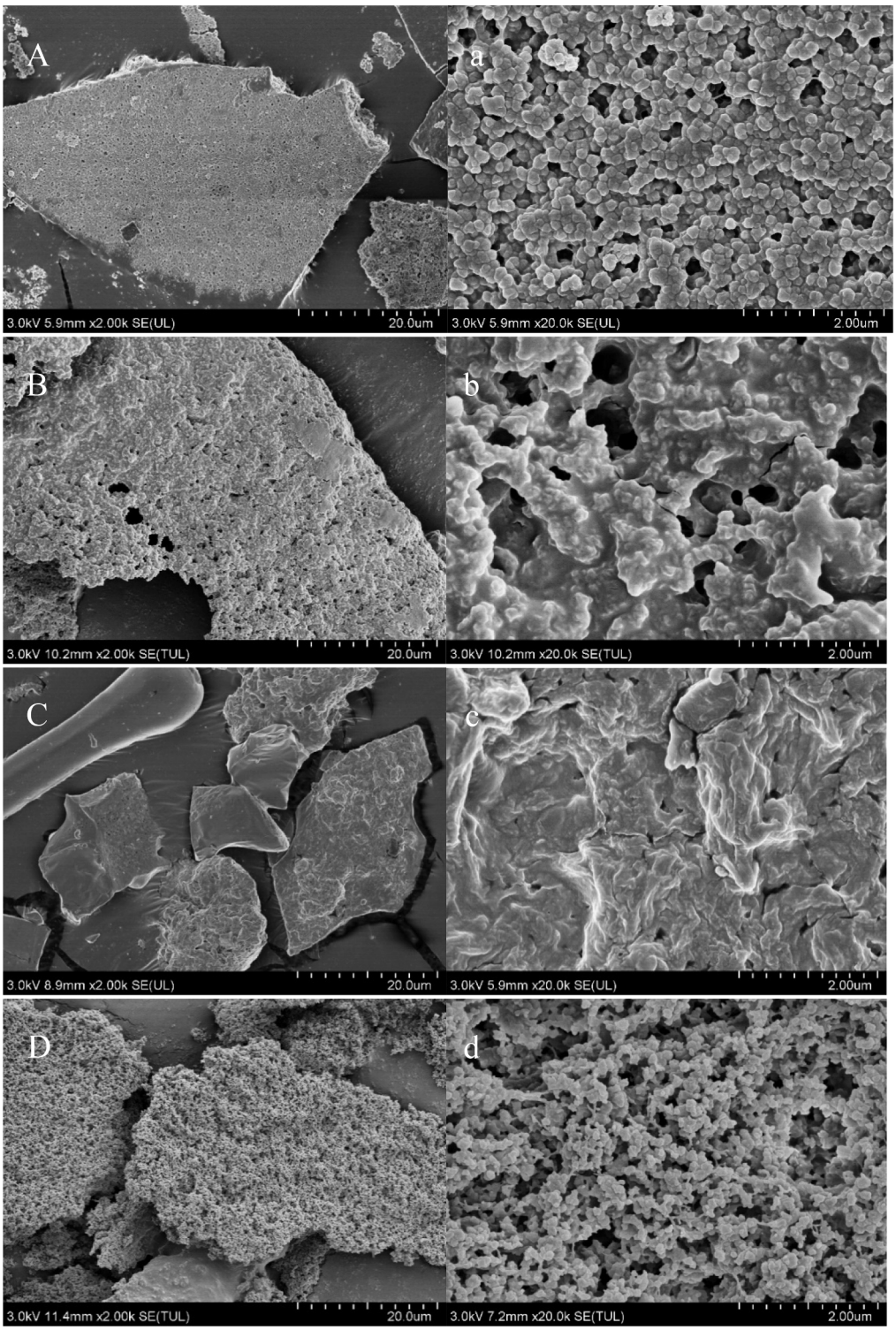

Fig. 1. Scanning electron microscopy images for W-SDF (A, a), C-SDF (B, b), A-SDF (C, c), E-SDF (D, d). W-SDF: soluble dietary fiber extracted by water; C-SDF: soluble dietary fiber extracted by acid; A-SDF: soluble dietary fiber extracted by alkali; E-SDF: soluble dietary fiber extracted by enzymes.

Feng, Niu, & Yu, 2018). The content of glucose in C-SDF increased compared to W-SDF, whereas other monosaccharides contents decreased, which was probably due to the strong destruction of the glycosidic bonds caused by the acid, resulting in the formation of glucose (Wang et al., 2021). C-SDF and E-SDF obtained a lower content of galactose than W-SDF, indicating that some side chains in galactose could be hydrolyzed by acid and enzyme extraction (Yuliarti et al., 2015). In addition, E-SDF had the highest content of uronic acid probably due to the hydrolyzation of carbohydrate chains and the crack of intermolecular hydrogen bonds, promoting the entry of uronic acid into the extract (Chen, Chen, et al., 2020). These results indicated that different extraction methods had minimal effects on the monosaccharide type of SDF but exerted considerable effects on the content of monosaccharide.

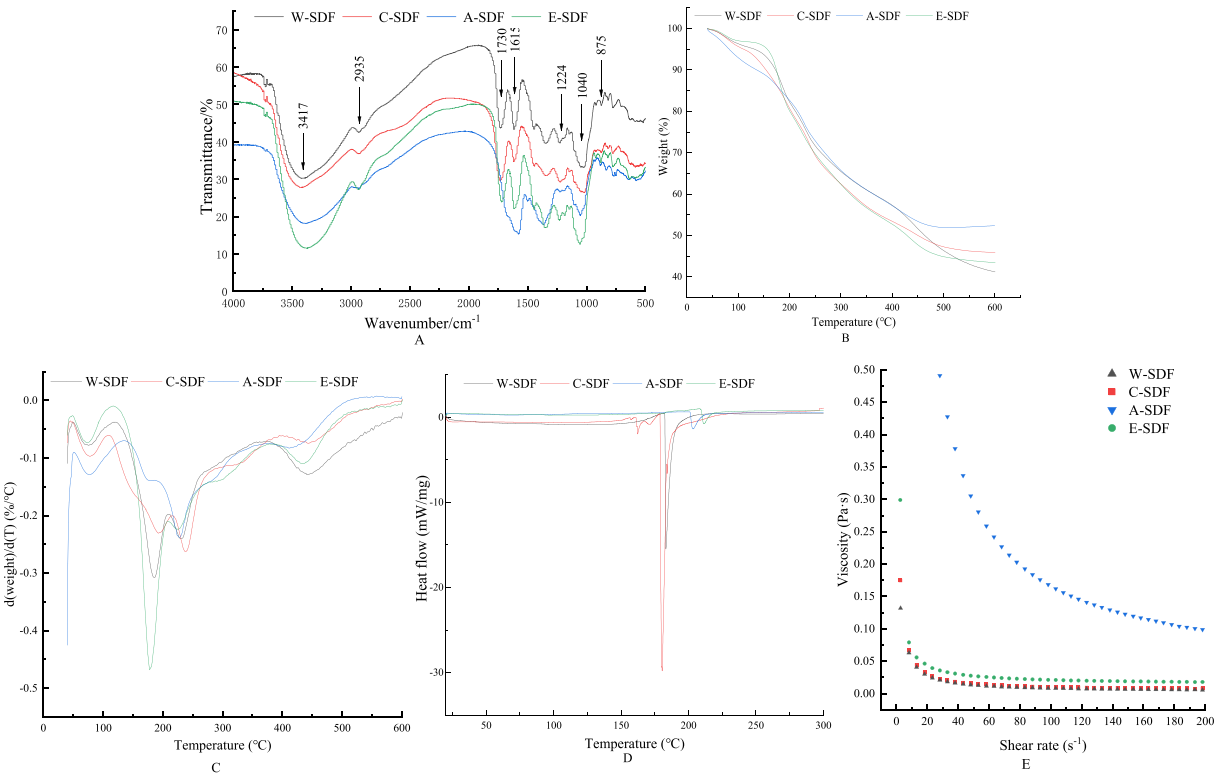

Fig. 2. FT-IR spectra (A), TGA curves (B), DTG curves (C), DSC curves (D) and apparent viscosity (E) of SDF samples extracted by different methods. SDF: soluble dietary fiber; W-SDF: soluble dietary fiber extracted by water; C-SDF: soluble dietary fiber extracted by acid; A-SDF: soluble dietary fiber extracted by alkali; E-SDF: soluble dietary fiber extracted by enzymes.

3.3. Molecular weight (M_W)

As displayed in Table 3, the molecular weight of SDF was detected by gel permeation chromatography. The average molecular weights of the SDF samples were 9.322 kDa (W-SDF), 8.421 kDa (C-SDF), 40.228 kDa (A-SDF) and 35.573 kDa (E-SDF), which were lower than the molecular weights of tomato peel SDF samples (Niu et al., 2018). Compared with M_W of W-SDF, that of A-SDF and E-SDF increased, whereas that of C-SDF decreased. The increase in M_W for A-SDF and E-SDF might be attributed to the specific effect of alkali and enzymes on glucoside bands, resulting in long carbohydrate chains (Du et al., 2021). As a polydispersity index, M_W/Mn indicates that a high index represents a wide molecular weight distribution (Li, Wang, Wang, & Xiong, 2016). The result showed that the molecular weight distribution of A-SDF and E-SDF was wider than W-SDF.

3.4. SEM analysis

The morphological structure of SDF was determined via SEM. As shown in Fig. 1, the structure of SDF subjected to different extraction methods varied. The surface of C-SDF was rougher than that of W-SDF, and the cellular structure of C-SDF was sparse. Numerous folds were found on the surface of A-SDF, on which the pores were fewer and more irregular. The decline of pore structure of C-SDF and A-SDF could be attributed to the damage of chemical reagent to pore structure of SDF (Huihan et al., 2023). Similar phenomena were also observed in the reported research (Wang et al., 2021). Furthermore, E-SDF had a poriferous surface, but the number of pores on E-SDF increased, and the pores became more compact and more regular than that of W-SDF indicating that enzymes could loosen the structure of SDF. In general, different extraction methods lead to various surface structures of SDF.

3.5. FT-IR

As presented in Fig. 2A, the structure of organic functional groups in SDF was investigated using an infrared spectrum. Four SDF samples roughly rendered the same spectrogram, but some differences were observed on particular peak sites. A strong and broad absorption peak, which arose from the stretching vibration of —OH, was observed around 3500–3250 cm^{-1}. The spectrum of E-SDF was enhanced compared to W-SDF and had a red shift phenomenon in this scope, indicating that additional hydrogen bonds were exposed in SDF after enzyme extraction. By contrast, the weaker peak intensity in A-SDF compared with that in W-SDF was likely due to the breakage of hydroxyl groups by alkali (Huang et al., 2021). The appearance of absorption peak in the range of 2950–2900 cm^{-1} was caused by the stretching vibration of C—H from methyl and methylene in the polysaccharide (Gan et al., 2020). The peak intensity of A-SDF weakened due to the rupture of molecular bonds induced by sodium hydroxide. In addition, the absorption peak of A-SDF disappeared at 1730 cm^{-1}, which is attributed to the ester carbonyl groups stretching of hemicellulose, lignin and pectin (Gu et al., 2020). Its disappearance occurred because the hydroxyl ions in alkaline solution disrupted the ester bonds. This phenomenon indicated that the alkaline solution hydrolyzed hemicellulose and lignin and de-esterified the pectin (Gu et al., 2020; Wandee et al., 2018). The absorption peak in the region of 1615 cm^{-1} was induced by the stretch of C═O in uronic acid, and the absorption intensity of C-SDF and A-SDF was weaker than that of W-SDF, suggesting that their uronic acid contents were low (Table 2) (Gu et al., 2020). The band around 1224 cm^{-1} indicated the vibration of C—O of the methoxy group in lignin and hemicellulose (Zhang et al., 2020). A decrease in this absorption peak of A-SDF further confirmed that hemicellulose and lignin were destroyed by alkali. The stretch of C—O—C and C—O—H in the sugar ring created the presence of the peak near 1040 cm^{-1} (Gan et al., 2020). A small peak around 875 cm^{-1} was related to the bending vibration of β-CH in the β-glycosidic

bond (Ding et al., 2020). Thus, the infrared spectrogram revealed that alkali extraction greatly affected the structure of SDF.

3.6. Thermal analysis

Thermal behavior was evaluated by TGA and DSC to ascertain the effect of different extraction methods on the thermal stability of SDF samples. As shown in Fig. 2B, the TGA curves presented how weight changed with temperature. A small decline in weight appeared between 40 °C and 150 °C due to the loss of free water and bound water (Gu et al., 2020). Rapid weight loss from 150 °C to 400 °C was due to the pyrolytic decomposition of polysaccharide (Gan et al., 2020). By contrast, the weight loss from 400 °C to 600 °C was due to the thermal decomposition of char (Wang et al., 2021). The residual weights of W-SDF, C-SDF, A-SDF and E-SDF were 41.22%, 45.95%, 52.34% and 43.47%, respectively. C-SDF, A-SDF and E-SDF all had higher residual weight compared with W-SDF, indicating that the heat stability of SDF samples extracted by acid, alkali and enzymes improved (Zhang et al., 2020). And the result showed that A-SDF had the highest residual weight, suggesting the thermal stability of A-SDF was the highest.

The DSC image in Fig. 2D shows the variation in heat flow against temperature from 0 °C to 300 °C. Two endothermic peaks around 180 °C belonged to C-SDF and W-SDF, and C-SDF had the lower peak temperature and the higher heat flow intensity than that of W-SDF accounting for the low heat stability of C-SDF (Kurek et al., 2018; Wang et al., 2015). The increased peak temperature and the decreased heat flow intensity of SDF after alkali and enzyme extraction illustrated that the heat stability of A-SDF and E-SDF was better than that of W-SDF. The peak temperature observed with C-SDF was the lowest among all samples, indicating that the water content of C-SDF was high (Table 1) (Iijimaa, Nakamuraa, Hatakeyamaa, & Hatakeyamab, 2000). The transformation temperature of four SDF samples exceeded 100 °C, suggesting that these SDF samples could be applied to various foods without interfering with the transition of the food matrix heated to the boiling point of water (Kurek et al., 2018). Differences in the peak temperature of SDF samples were observed, suggesting that the four SDF samples extracted by different methods had no homogeneity in structure (Moczkowska et al., 2019). In summary, the alkali and enzyme extraction methods improved the heat stability of SDF. Therefore, both methods could effectively alter the structure of SDF and affect its properties.

3.7. Particle size and ζ-potential

The particle size and ζ-potential of SDF samples were determined, because hydrodynamic particles and polysaccharide charges can reflect the stability of the solution to some extent (Chen, Hong, Ji, Wu, & Ma, 2020). The particle size of the four SDF samples is exhibited in Table 3. E-SDF presented the largest particle size, followed by W-SDF and C-SDF, whereas the particle size of A-SDF was the smallest. The significant reduction ($p < 0.05$) in particle size may have resulted from the elimination of lignin and some alcohol-soluble substances caused by alkali (Huang et al., 2021). A decrease in the particle size of A-SDF could inhibit SDF aggregation, thereby improving the stability of food emulsions (Ketenoglu, Mert, & Tekin, 2014).

ζ-Potential was used to depict the surface charge of SDF molecules. As shown in Table 3, the ζ-potential of SDF samples extracted by the four methods showed significant differences ($p < 0.05$). The surface charges of the four SDF samples were all negative charges, and A-SDF had the most negative charges. A-SDF with the most negative charges resulted from the conversion of the free carboxylic groups into ionized carboxylic groups under alkaline conditions (Yan et al., 2021). SDF with many negative charges had strong electrostatic attraction, resulting in high gelation ability (Niu et al., 2018). The high absolute value of ζ-potential indicates that the solution has a good stability. This is because the molecules more strongly repel each other due to more charges, making the particles in the system less likely to aggregate (Huang et al., 2021). In addition, the solution is generally considered to be stable when ζ-potential is lower than −30 mV (Liu, Shim, Shen, Wang, Ghosh, & Reaney, 2016). In summary, A-SDF and E-SDF presented good stability in solution and gelling ability.

3.8. Apparent viscosity

As shown in Fig. 2E, the viscosity of SDF samples all decreased with the increase in shear rate, indicating that SDF is a pseudoplastic fluid with shear-thinning behavior. Shear-thinning behavior was attributed to the destruction of the entanglement between the molecules caused by shear force, making the molecules array along the flow direction. Moreover, the apparent viscosity decreased with the increase in shear rate (Yan et al., 2021). The viscosity of C-SDF was similar to that of W-SDF, and the viscosity of E-SDF increased slightly, whereas the viscosity of A-SDF improved dramatically. A-SDF had high viscosity probably due to high molecular weight in A-SDF, because A-SDF with high molecular weight can contribute to the entanglement of the molecule, resulting in the high viscosity of A-SDF (Niu et al., 2018). The increase in molecular surface charge thickens the dissolved layer of the molecule, leading to the further extension of the molecule, so the apparent viscosity of the solution increases (Wang et al., 2019). The viscosity of A-SDF increased probably because A-SDF had more negative charges than other SDF samples (Table 3). A-SDF with high viscosity could be used as a thickener, gelatinizing agent, texture modifier, suspending agent, and stabilizer for application in food (Liu et al., 2016). For instance, dietary fiber with shear-thinning behavior can be used as thickener for drinks (Zhang et al., 2018).

3.9. Functional properties

3.9.1. Water solubility (WS) and oil holding capacity (OHC)

As shown in Table 3, no significant differences ($p > 0.05$) were found in WS among the four SDF samples, indicating that acid, alkali and enzymes had minimal impact on WS of SDF. Four SDF samples had high WS (85%–93%), and the result was higher than the WS of 12 varieties of pomegranate SDF (47.87%–65.00%) (Hasnaoui et al., 2014). In addition, high WS benefits application in food, such as bread and drinks (Ding et al., 2020).

The OHC of dietary fiber is important in food application, such as the preservation of flavor and fat in food (Lv, Liu, Zhang, & Wang, 2017; Wang, Zhang, Xiao, Huang, Li, & Fu, 2018). Compared with W-SDF, the OHC of SDF samples significantly improved ($p < 0.05$) after extraction by acid, alkali and enzymes. The highest OHC (5.36 g/g) of E-SDF was higher than that of SDF extracted by enzymes from the peel of 12 varieties of pomegranate (2.80–4.05 mL/g) (Hasnaoui et al., 2014), probably due to the differences in enzymes used during extraction or varieties of pomegranate. The highest OHC of E-SDF may be attributed to the dense porous structure in E-SDF (Fig. 1d). SDF with a porous structure has a higher contact area with oil and has more exposed functional groups; thus, the oil easily penetrates into SDF (Jia et al., 2019). E-SDF with high OHC can stabilize oil-rich emulsion products and ameliorate the cooking performance of meat products, such as beef sausage (Ketenoglu et al., 2014). Therefore, E-SDF has the potential to be applied as an additive to oil-rich foods.

3.9.2. Glucose adsorption capacity (GAC)

The adsorption capacity of dietary fiber to glucose can postpone the absorption of glucose in the gastrointestinal tract, thereby reducing postprandial blood glucose (Yu, Bei, Zhao, Li, & Cheng, 2018). The amount of glucose bound to the sample increased with increasing glucose concentration. No significant difference ($p > 0.05$) was found between E-SDF and W-SDF in the GAC, and the GAC of E-SDF and W-SDF was the highest. This result may be related to more pore structures and uronic acid in E-SDF and W-SDF, leading to larger superficial areas and

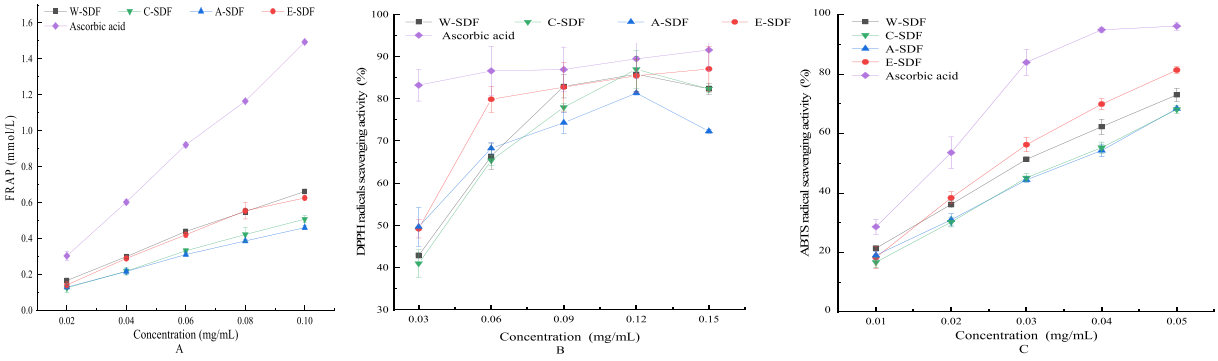

Fig. 3. In vitro antioxidant activities of SDF samples extracted by different methods: ferric reducing antioxidant power (A); DPPH radical scavenging activity (B); ABTS radical scavenging activity (C). SDF: soluble dietary fiber; W-SDF: soluble dietary fiber extracted by water; C-SDF: soluble dietary fiber extracted by acid; A-SDF: soluble dietary fiber extracted by alkali; E-SDF: soluble dietary fiber extracted by enzymes.

more aldehyde acid functional groups to adsorb glucose (Gu et al., 2020). Therefore, SDF extracted by enzymes had better adsorption capacity to glucose than C-SDF and A-SDF.

3.9.3. *In vitro antioxidant activities*

As shown in Fig. 3A, 3B and 3C, ferric reducing antioxidant power (FRAP) and radical scavenging capacity are representatives of antioxidant activities. Antioxidants exhibit the antioxidant power by reducing the ferric (Fe^{3+}) form to the ferrous (Fe^{2+}) form and donating hydrogen or electrons to the radical (Meng, Liu, Xiao, Cao, Wang, & Duan, 2019). FRAP and scavenging ability on DPPH and ABTS radicals of all samples were lower than that of the positive control ascorbic acid. The FRAP of four SDF samples was denoted by the concentration of ferrous sulfate (0.02–0.10 mg/mL) and improved with the increase in sample concentration. C-SDF and A-SDF possessed lower FRAP compared with W-SDF, whereas the FRAP of E-SDF was similar with that of W-SDF. The DPPH radical scavenging activity at 0.15 mg/mL were 82.36%, 82.35%, 72.30% and 87.07% for W-SDF, C-SDF, A-SDF and E-SDF, respectively. The ABTS radical scavenging activity of SDF samples presented a concentration-dependent trend in different concentrations (0.01–0.05 mg/mL). The ABTS radical scavenging activity of E-SDF was higher than that of W-SDF, whereas the scavenging activity of C-SDF and A-SDF was lower than that of W-SDF. Overall, we observed that E-SDF possessed the highest antioxidant capacity compared with C-SDF and A-SDF as a consequence of more pore structures (Fig. 1), higher content of uronic acid (Table 2) and higher content of hydroxyl groups (Fig. 2A). Pore structures can promote the exposure of the inhibited sites. Aldehydes in uronic acid, as an electrophilic groups, can promote the dissociation of hydrogen in the O—H bond (Wang, Hu, Nie, Yu, & Xie, 2016). And hydroxyl groups can provide electron or hydrogens to free radical (Lu, Li, Jin, Li, Yi, & Huang, 2019). In addition, the ratio of different monosaccharides and molecular weight have effects on the antioxidant activity (Lo, Chang, Chiu, Tsay, & Jen, 2011; Wang, Hu, et al., 2016).

4. Conclusion

We adopted different extraction methods, namely, acid extraction, alkali extraction and enzyme extraction, to extract SDF from pomegranate peel. Results showed that alkali and enzyme extraction improved the SDF yield compared with water extraction, and glucose was the primary monosaccharide in all SDF samples. A-SDF and E-SDF showed higher molecular weight and better thermal stability than W-SDF. The dense structure and honeycomb structure were found in A-SDF and E-SDF, respectively. Due to the introduction of hydroxyl ions in the sample under alkali extraction, the functional group structure of A-SDF was changed. In addition, A-SDF exhibited the lowest ζ-potential, smallest particle size and highest viscosity, and it can be used as food additive. E-SDF possessed better OHC so it could be an option to be added as an additive in oil-rich foods and had better in vitro antioxidant capacity than C-SDF and A-SDF. The differences in the functional characteristics of the samples were attributed to the discrepancies in their structures and physicochemical properties. Nevertheless, the application in food processing and in vivo physiological properties of pomegranate peel SDF require further research.

CRediT authorship contribution statement

Min Xiong: Conceptualization, Writing – original draft, Validation. **Mei Feng:** Writing – original draft, Validation. **Yanli Chen:** Validation. **Zhengfeng Fang:** Data curation. **Lina Wang:** Data curation. **Derong Lin:** Data curation. **Qing Zhang:** Data curation. **Yuntao Liu:** Writing – review & editing. **Yuheng Luo:** Writing – review & editing. **Hong Chen:** Conceptualization, Writing – review & editing.

Declaration of Competing Interest

The authors declare that they have no known competing financial interests or personal relationships that could have appeared to influence the work reported in this paper.

Data availability

No data was used for the research described in the article.

Acknowledgments

This work was supported by the Key Laboratory of Agricultural Product Processing and Nutrition Health (Co-construction by Ministry and Province), Ministry of Agriculture and Rural Affairs.

References

Bader Ul Ain, H., Saeed, F., Ahmed, A., Asif Khan, M., Niaz, B., & Tufail, T. (2019). Improving the physicochemical properties of partially enhanced soluble dietary fiber through innovative techniques: A coherent review. *Journal of Food Processing and Preservation, 43*(4). doi: 10.1111/jfpp.13917.

Chen, G., Hong, Q., Ji, N., Wu, W., & Ma, L. (2020). Influences of different drying methods on the structural characteristics and prebiotic activity of polysaccharides from bamboo shoot (Chimonobambusa quadrangularis) residues. *International Journal of Biological Macromolecules, 155*, 674–684. https://doi.org/10.1016/j.ijbiomac.2020.03.223

Chen, H., Xiong, M., Bai, T., Chen, D., Zhang, Q., Lin, D., et al. (2021). Comparative study on the structure, physicochemical, and functional properties of dietary fiber extracts from quinoa and wheat. *Lwt, 149*. https://doi.org/10.1016/j.lwt.2021.111816

Chen, X., Chen, G., Wang, Z., & Kan, J. (2020). A comparison of a polysaccharide extracted from ginger (Zingiber officinale) stems and leaves using different methods: Preparation, structure characteristics, and biological activities. *International Journal of Biological Macromolecules, 151*, 635–649. https://doi.org/10.1016/j.ijbiomac.2020.02.222

Cheng, L., Zhang, X., Hong, Y., Li, Z., Li, C., & Gu, Z. (2017). Characterisation of physicochemical and functional properties of soluble dietary fibre from potato pulp

obtained by enzyme-assisted extraction. *International Journal of Biological Macromolecules, 101*, 1004–1011. https://doi.org/10.1016/j.ijbiomac.2017.03.156
Ding, Q., Li, Z., Wu, W., Su, Y., Sun, N., Luo, L., et al. (2020). Physicochemical and functional properties of dietary fiber from Nannochloropsis oceanica: A comparison of alkaline and ultrasonic-assisted alkaline extractions. *Lwt, 133*. https://doi.org/10.1016/j.lwt.2020.110080
Du, X., Wang, L., Huang, X., Jing, H., Ye, X., Gao, W., et al. (2021). Effects of different extraction methods on structure and properties of soluble dietary fiber from defatted coconut flour. *Lwt, 143*. https://doi.org/10.1016/j.lwt.2021.111031
Gan, J., Huang, Z., Yu, Q., Peng, G., Chen, Y., Xie, J., et al. (2020). Microwave assisted extraction with three modifications on structural and functional properties of soluble dietary fibers from grapefruit peel. *Food Hydrocolloids, 101*. https://doi.org/10.1016/j.foodhyd.2019.105549
Gu, M., Fang, H., Gao, Y., Su, T., Niu, Y., & Yu, L. (2020). Characterization of enzymatic modified soluble dietary fiber from tomato peels with high release of lycopene. *Food Hydrocolloids, 99*. https://doi.org/10.1016/j.foodhyd.2019.105321
Hasnaoui, N., Wathelet, B., & Jimenez-Araujo, A. (2014). Valorization of pomegranate peel from 12 cultivars: Dietary fibre composition, antioxidant capacity and functional properties. *Food Chemistry, 160*, 196–203. https://doi.org/10.1016/j.foodchem.2014.03.089
Huang, J., Liao, J., Qi, J., Jiang, W., & Yang, X. (2021). Structural and physicochemical properties of pectin-rich dietary fiber prepared from citrus peel. *Food Hydrocolloids, 110*. https://doi.org/10.1016/j.foodhyd.2020.106140
Hui, L., Fusheng, C., Hongshun, Y., Yongzhi, Y., Xiangzhe, G., Ying, X., et al. (2009). Effect of calcium treatment on nanostructure of chelate-soluble pectin and physicochemical and textural properties of apricot fruits. *Food Research International, 42*(8). https://doi.org/10.1016/j.foodres.2009.05.014
Huihan, X., Aixia, W., Wanyu, Q., Mengzi, N., Zhiying, C., Yue, H., et al. (2023). The structural and functional properties of dietary fibre extracts obtained from highland barley bran through different steam explosion-assisted treatments. *Food Chemistry, 406*. https://doi.org/10.1016/j.foodchem.2022.135025
Iijimaa, M., Nakamuraa, K., Hatakeyamaa, T., & Hatakeyamab, H. (2000). Phase transition of pectin with sorbed water. *Carbohydrate Polymers, 41*(1), 101–106. https://doi.org/10.1016/S0144-8617(99)00116-2
Jia, M., Chen, J., Liu, X., Xie, M., Nie, S., Chen, Y., et al. (2019). Structural characteristics and functional properties of soluble dietary fiber from defatted rice bran obtained through Trichoderma viride fermentation. *Food Hydrocolloids, 94*, 468–474. https://doi.org/10.1016/j.foodhyd.2019.03.047
Ketenoglu, O., Mert, B., & Tekin, A. (2014). Effects of microfluidized dietary fibers on stability properties of emulsions. *Journal of Texture Studies, 45*(4), 295–306. https://doi.org/10.1111/jtxs.12074
Kurek, M. A., Karp, S., Wyrwisz, J., & Niu, Y. (2018). Physicochemical properties of dietary fibers extracted from gluten-free sources: Quinoa (Chenopodium quinoa), amaranth (Amaranthus caudatus) and millet (Panicum miliaceum). *Food Hydrocolloids, 85*, 321–330. https://doi.org/10.1016/j.foodhyd.2018.07.021
Langley-Evans, S. C. (2000). Antioxidant potential of green and black tea determined using the ferric reducing power (FRAP) assay. *International Journal of Food Sciences and Nutrition, 51*(3), 181–188. https://doi.org/10.1080/09637480050029683
Li, N., Feng, Z., Niu, Y., & Yu, L. (2018). Structural, rheological and functional properties of modified soluble dietary fiber from tomato peels. *Food Hydrocolloids, 77*, 557–565. https://doi.org/10.1016/j.foodhyd.2017.10.034
Li, X., Wang, L., Wang, Y., & Xiong, Z. (2016). Effect of drying method on physicochemical properties and antioxidant activities of Hohenbuehelia serotina polysaccharides. *Process Biochemistry, 51*(8), 1100–1108. https://doi.org/10.1016/j.procbio.2016.05.006
Liu, J., Shim, Y., Shen, J., Wang, Y., Ghosh, S., & Reaney, M. J. T. (2016). Variation of composition and functional properties of gum from six Canadian flaxseed (Linum usitatissimum L.) cultivars. *International Journal of Food Science & Technology, 51*(10), 2313–2326. https://doi.org/10.1111/ijfs.13200
Lo, T. C. T., Chang, C. A., Chiu, K. H., Tsay, P. K., & Jen, J. F. (2011). Correlation evaluation of antioxidant properties on the monosaccharide components and glycosyl linkages of polysaccharide with different measuring methods. *Carbohydrate Polymers, 86*(1), 320–327. https://doi.org/10.1016/j.carbpol.2011.04.056
Lu, J., Li, J., Jin, R., Li, S., Yi, J., & Huang, J. (2019). Extraction and characterization of pectin from Premna microphylla Turcz leaves. *International Journal of Biological Macromolecules, 131*, 323–328. https://doi.org/10.1016/j.ijbiomac.2019.03.056
Lv, J., Liu, X., Zhang, X., & Wang, L. (2017). Chemical composition and functional characteristics of dietary fiber-rich powder obtained from core of maize straw. *Food Chemistry, 227*, 383–389. https://doi.org/10.1016/j.foodchem.2017.01.078
Meng, X., Liu, F., Xiao, Y., Cao, J., Wang, M., & Duan, X. (2019). Alterations in physicochemical and functional properties of buckwheat straw insoluble dietary fiber by alkaline hydrogen peroxide treatment. *Food Chemistry, 3*, Article 100029. https://doi.org/10.1016/j.fochx.2019.100029
Meng, X., Wu, C., Liu, H., Tang, Q., & Nie, X. (2021). Dietary fibers fractionated from gardenia (Gardenia jasminoides Ellis) husk: Structure and in vitro hypoglycemic effect. *Journal of the Science of Food and Agriculture, 101*(9), 3723–3731. https://doi.org/10.1002/jsfa.11003
Moczkowska, M., Karp, S., Niu, Y., & Kurek, M. A. (2019). Enzymatic, enzymatic-ultrasonic and alkaline extraction of soluble dietary fibre from flaxseed – A physicochemical approach. *Food Hydrocolloids, 90*, 105–112. https://doi.org/10.1016/j.foodhyd.2018.12.018
Niu, Y., Li, N., Xia, Q., Hou, Y., & Xu, G. (2018). Comparisons of three modifications on structural, rheological and functional properties of soluble dietary fibers from tomato peels. *LWT - Food Science and Technology, 88*, 56–63. https://doi.org/10.1016/j.lwt.2017.10.003
O'Shea, N., Arendt, E. K., & Gallagher, E. (2012). Dietary fibre and phytochemical characteristics of fruit and vegetable by-products and their recent applications as novel ingredients in food products. *Innovative Food Science & Emerging Technologies, 16*, 1–10. https://doi.org/10.1016/j.ifset.2012.06.002
Wandee, Y., Uttapap, D., & Mischnick, P. (2018). Yield and structural composition of pomelo peel pectins extracted under acidic and alkaline conditions. *Food Hydrocolloids, 87*, 237–244. https://doi.org/10.1016/j.foodhyd.2018.08.017
Wang, H., Liu, S., Zhou, X., Yang, X., Gao, Q., Tanokura, M., et al. (2019). Treatment with hydrogen peroxide improves the physicochemical properties of dietary fibres from Chinese yam peel. *International Journal of Food Science & Technology, 55*(3), 1289–1297. https://doi.org/10.1111/ijfs.14405
Wang, J., Hu, S., Nie, S., Yu, Q., & Xie, M. (2016). Reviews on Mechanisms of In Vitro Antioxidant Activity of Polysaccharides. *Oxidative Medicine and Cellular Longevity, 2016*. https://doi.org/10.1155/2016/5692852
Wang, K., Li, M., Wang, Y., Liu, Z., & Ni, Y. (2021). Effects of extraction methods on the structural characteristics and functional properties of dietary fiber extracted from kiwifruit (Actinidia deliciosa). *Food Hydrocolloids, 110*. https://doi.org/10.1016/j.foodhyd.2020.106162
Wang, L., Xu, H., Yuan, F., Fan, R., & Gao, Y. (2015). Preparation and physicochemical properties of soluble dietary fiber from orange peel assisted by steam explosion and dilute acid soaking. *Food Chemistry, 185*, 90–98. https://doi.org/10.1016/j.foodchem.2015.03.112
Wang, L., Zhang, B., Xiao, J., Huang, Q., Li, C., & Fu, X. (2018). Physicochemical, functional, and biological properties of water-soluble polysaccharides from Rosa roxburghii Tratt fruit. *Food Chemistry, 249*, 127–135. https://doi.org/10.1016/j.foodchem.2018.01.011
Wang, N., Zhang, Y., Wang, X., Huang, X., Fei, Y., Yu, Y., et al. (2016). Antioxidant property of water-soluble polysaccharides from Poria cocos Wolf using different extraction methods. *International Journal of Biological Macromolecules, 83*, 103–110. https://doi.org/10.1016/j.ijbiomac.2015.11.032
Xiong, M., Zheng, S., Bai, T., Chen, D., Qin, W., Zhang, Q., et al. (2022). The difference among structure, physicochemical and functional properties of dietary fiber extracted from triticale and hull-less barley. *Lwt, 154*. https://doi.org/10.1016/j.lwt.2021.112771
Yan, J., Wang, C., Qiu, W., Chen, T., Yang, Y., Wang, W., et al. (2021). Ultrasonic treatment at different pH values affects the macromolecular, structural, and rheological characteristics of citrus pectin. *Food Chemistry, 341*(Pt 1), Article 128216. https://doi.org/10.1016/j.foodchem.2020.128216
Yu, G., Bei, J., Zhao, J., Li, Q., & Cheng, C. (2018). Modification of carrot (Daucus carota Linn. var. Sativa Hoffm.) pomace insoluble dietary fiber with complex enzyme method, ultrafine comminution, and high hydrostatic pressure. *Food Chemistry, 257*, 333–340. https://doi.org/10.1016/j.foodchem.2018.03.037
Yuliarti, O., Goh, K. K., Matia-Merino, L., Mawson, J., & Brennan, C. (2015). Extraction and characterisation of pomace pectin from gold kiwifruit (Actinidia chinensis). *Food Chemistry, 187*, 290–296. https://doi.org/10.1016/j.foodchem.2015.03.148
Zhang, H., Zhang, N., Xiong, Z., Wang, G., Xia, Y., Lai, P., et al. (2018). Structural characterization and rheological properties of beta-D-glucan from hull-less barley (Hordeum vulgare L. var. nudum Hook. f.). *Phytochemistry, 155*, 155–163. https://doi.org/10.1016/j.phytochem.2018.08.004
Zhang, Y., Qi, J., Zeng, W., Huang, Y., & Yang, X. (2020). Properties of dietary fiber from citrus obtained through alkaline hydrogen peroxide treatment and homogenization treatment. *Food Chemistry, 311*, Article 125873. https://doi.org/10.1016/j.foodchem.2019.125873
Zheng, Y., Wang, X., Tian, H., Li, Y., Shi, P., Guo, W., et al. (2021). Effect of four modification methods on adsorption capacities and in vitro hypoglycemic properties of millet bran dietary fibre. *Food Research International, 147*, Article 110565. https://doi.org/10.1016/j.foodres.2021.110565